P9.11 Using Satellite-based Lightning Products to Enhance Aviation Decision Support Systems: A Feasibility Study

Cathy Kessinger, Wiebke Deierling, John K. Williams, Robert Sharman, Nancy Rehak and Jason Craig

National Center for Atmospheric Research – Research Applications Laboratory

Introduction

Predicting the intensity, location and timing of convection initiation and extrapolation of existing storms is a difficult endeavor over oceanic regions that are far-removed from land and have few surface-based observations. Geostationary and Low Earth Orbit (LEO) satellites can be the primary and sometimes exclusive source of observations. The feasibility of improving the diagnosis and nowcasting of aviation hazards related to deep convection (oceanic or continental) is examined using the National Aeronautics and Space Administration (NASA) satellite measurements of brightness temperatures, total lightning and ice water path. Further, inferred lightning estimates are examined as a diagnostic tool. Data from the Defense Meteorological Satellite Program (DMSP) satellites will be used in the future.

The presence of lightning indicates that a storm has attained at least the minimum updraft strength to be an aviation hazard. Strong updrafts imply that aviation hazards such as turbulence, wind shear and icing may be present. Brightness temperatures and ice water path as derived from instruments onboard the Tropical Rainfall Measuring Mission (TRMM; Blyth et al. 2001; Petersen et al. 2005) are uniquely related to total lightning activity and can be used as input to improve convection diagnosis and nowcasting results. Investigation into potential relationships between cloud-to-ground (CG) lightning measurements and convectively-induced turbulence are examined to determine their potential use for global turbulence detection.

Case Study Data – 28 May 2008

A case study from 28 May 2008 is selected to examine the relationships between lightning and aviation hazards. The NEXRAD radar mosaic (Fig. 1) shows convection is present along a frontal boundary located across the southeastern United States. The domain for the case study of interest is at the westernmost portion of the convective system (red box). The 1800 UTC (all times UTC) TRMM overflight swath is shown by the Visible and Infrared Scanner (VIRS) image that underlays the reflectivity.

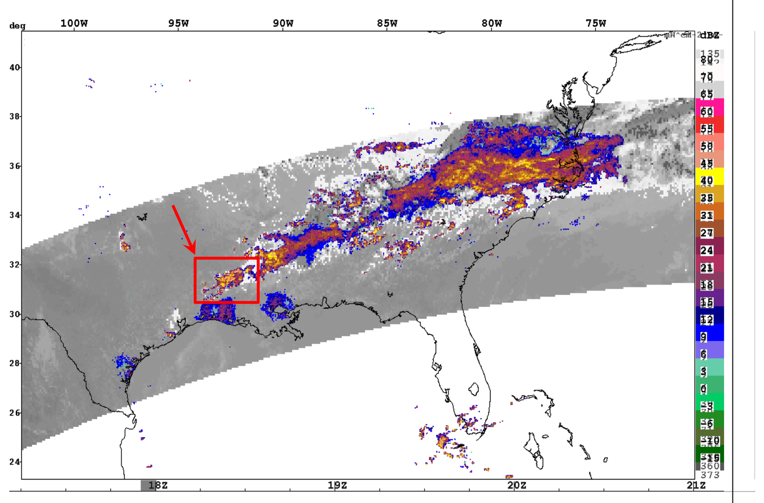

Figure 1. NEXRAD composite reflectivity (dBZ) mosaic is overlaid onto the TRMM VIRS 10.8 micron channel and shows the TRMM overpass region at 1800 UTC. The case study domain is indicated by the red box.

The NEXRAD radar mosaic is shown for four times (Fig. 2) that bracket various stages of convective development of the selected portion of the convective system. In Fig. 2a, the first radar returns from a cell (labeled "A") are seen at 1520. An hour later at 1620 (Fig. 2b), the first cloud-to-ground lightning flash is observed within the National Lightning Detection Network (NLDN). At 1800 (Fig. 2c), the convective system has continued to evolve and numerous NLDN flashes are observed within the convective cells. Also at this time, the TRMM overflight occurs over the area. By 1925 (Fig. 2d), the convective system has continued to expand towards the west with convective cores producing numerous lightning flashes.

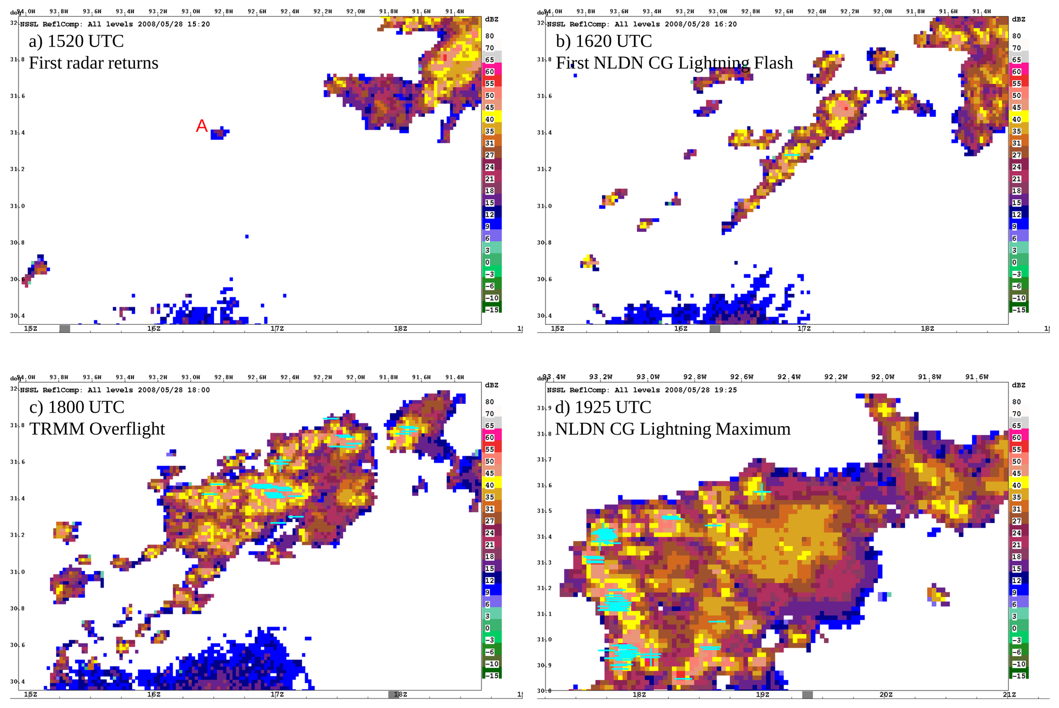

Figure 2. The National Severe Storms Laboratory (NSSL) composite reflectivity (dBZ) mosaic is shown with the location of NLDN cloud-to-ground flashes at four times: a) 1520, b) 1620, c) 1800 and d) 1925 UTC on 28 May 2008. Note the first NLDN cloud-to-ground flash occurred at 1620 UTC. The times shown correspond to the red, vertical dashed lines in Fig. 3. The location of this domain (Fig. 1) is within the southeastern United States.

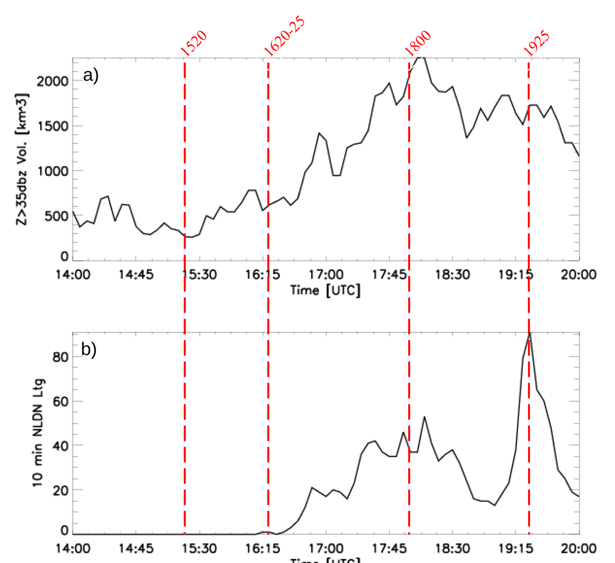

Figure 3. Time series plots from 1400 to 2000 UTC on 28 May 2008. Values are computed over the case study domain shown in Fig. 2. Fields plotted include a) the volume (km^3) of reflectivity $\geq$35 dBZ at and above the -10^{o}C level and b) the number of cloud-to-ground lightning flashes measured by the NLDN over the previous 10 min. The times corresponding to panels in Fig. 2 are shown by the vertical, dashed red lines.

The time series plots (Fig. 3) show the evolution of the volume of reflectivity $\geq$35 dBZ above the -10^{o}C vertical level and the number of NLDN lightning flashes over the previous 10 min period. At 1520, the volume of reflectivity in the system is at a minimum (compare Fig. 3a to Fig. 2a). The period between 1520 and 1800 is marked by initiation and growth of convective cells and by increasing lightning activity with the first cloud-to-ground flash occurring at 1620 (compare Fig. 2b to 2c). After 1800, the convective volume begins a gradual decrease as does the number of lightning flashes until ~1900. The maximum number of flashes observed quickly follows at 1925 (Fig. 3b), exceeding the number of flashes seen earlier by a significant margin, and corresponds to convective redevelopment in the western edge of the domain (Fig. 2d). At this time, the earlier storms are dissipating.

Using 37 and 85 GHz TMI Channels to Infer Lightning Potential

On 28 May 2008, the TRMM satellite did an overflight of the case study region at 1759 UTC. Figure 1 shows the swath location. Measurements from the TRMM instruments allow additional insights into the microphysical processes within the storm that contribute to storm electrification. Data sets are available from the TRMM Microwave Imager (TMI), the Precipitation Radar (PR), the VIRS and the Lightning Imaging Sensor (LIS). Figure 4 shows the number of lightning groups observed by the LIS within the outline of the convective system reflectivity at 20 dBZ. While the LIS measures an important metric of storm electrification, its viewing time is approximately 90 seconds over any location. The quantity of total lightning that a deep convective storm can produce has been documented to have large fluctuations within a few minutes. Deriving lightning amounts from satellite brightness temperatures may yield a more temporally smoothed storm potential for hazardous lightning production.

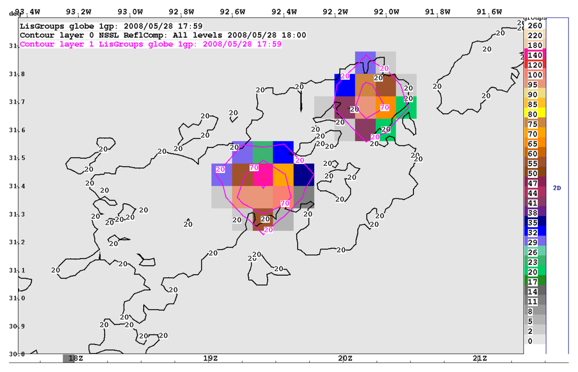

Figure 4. The number of lightning groups observed by LIS are shown at 1759 UTC on 28 May 2008 for the case study. The number of groups are shaded and contoured to better show the values. The composite reflectivity is contoured at 20 dBZ.

From the TMI, the satellite brightness temperatures (T_B) at 37 and 85 GHz are polarization corrected (PCT), following Cecil et al. (2002) and Spencer et al. (1989). The corrected brightness temperatures are then input into equations derived by Blyth et al. (2001) that relate brightness temperature to lightning activity (L) when the number of lightning groups exceed 20/min. These equations are:

$$T_B(37\ GHz) = 330 - 45 \log(L), \text{ where } L>20 \text{ groups/min} \quad (1)$$

$$T_B(85\ GHz) = 330 - 70 \log(L), \text{ where } L>20 \text{ groups/min} \quad (2)$$

Blyth et al. (2001) found that these relationships are valid for convective storms having both continental and maritime origins. Good correspondence is found (Fig. 5) in the location of the derived lightning groups and the observed LIS groups within the storm. Differences are seen in the maximum number of groups when comparing the derived and observed values. While a one-to-one correspondence to LIS values is not expected, these derived quantities show that the storm is electrically active.

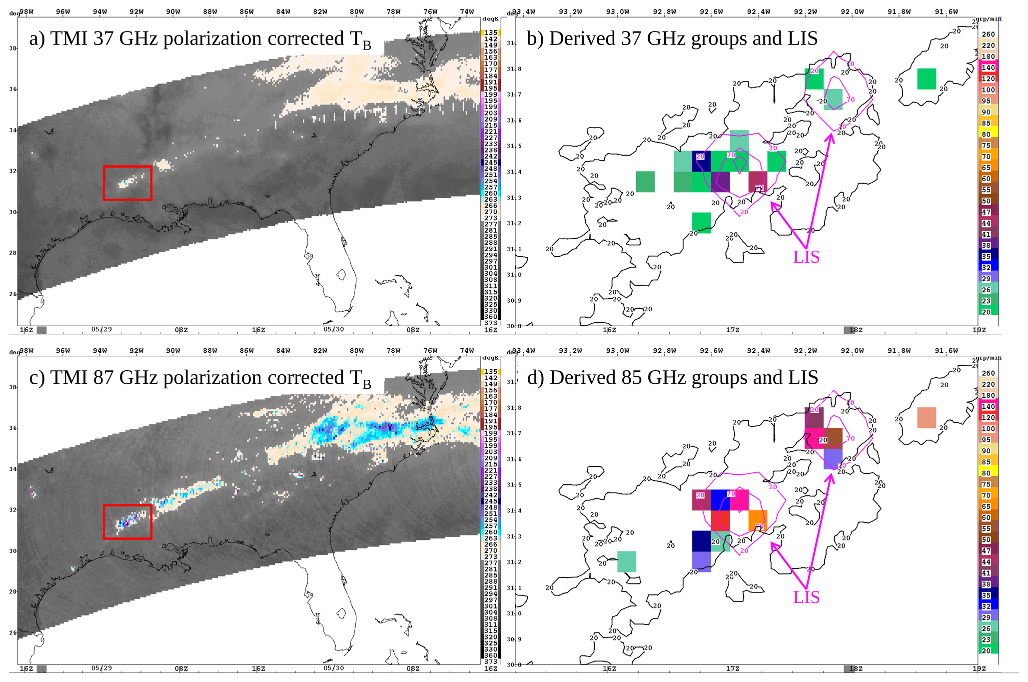

Figure 5. This plot shows the a) TMI polarization corrected brightness temperatures at 37 GHz and b) the derived number of lightning groups from Eq. 1, the number of LIS groups (magenta contours) and the 20 dBZ composite reflectivity contour (black line). Likewise, c) and d) show the same fields for the TMI 85 GHz data with the number of lightning groups computed from Eq. 2. Date and time shown are 28 May 2008 at 1759 UTC.

Using Derived Lightning Groups within Oceanic Convection Diagnostic

A fuzzy logic, data fusion technique, described in Kessinger et al. (2010), diagnoses the presence of deep convection using geostationary satellite imagery over oceanic regions where ground-based data sets are limited. While not fully described here, this technique is augmented with the derived 37 GHz and 85 GHz lightning groups (Fig. 5) for the purposes of illustrating how these fields may assist in better pinpointing regions of convective hazards.

Briefly, the Convective Diagnosis Oceanic (CDO) technique combines multiple, scaled input fields in a weighted summation and is then normalized. The output is an interest field (values between 0 and 1) that indicates the likelihood of convection with values $\geq$0.5 interest defining deep convection. Several configurations of the CDO are run for concept testing. In Fig. 6a, the CDO is computed using inputs from geostationary satellite imagery. In Fig. 6b, the CDO includes the 37 GHz derived lightning group as an input field. Likewise, in Fig. 6c, the CDO inputs the 85 GHz derived lightning group. Each CDO configuration is compared (Fig. 7) with corresponding composite reflectivity and NLDN flashes (Fig. 7a) and the reflectivity at 5.5 km (Fig. 7b). Results suggest some improvement is realized in CDO performance with the addition of these two lightning group fields. Additional work is planned to validate these preliminary results.

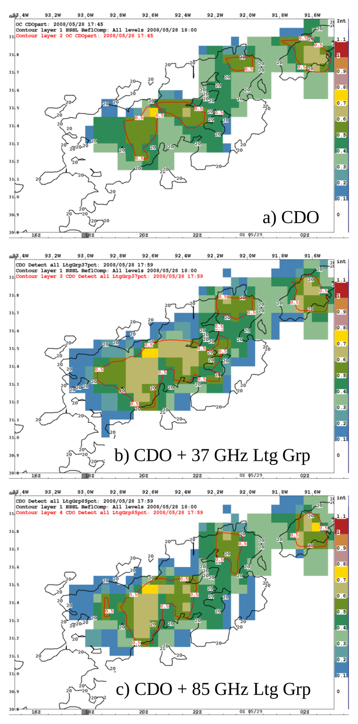

Figure 6. The CDO is computed 3 ways with the 0.5 interest contoured (red line). The 20 dBZ reflectivity contour is shown (black line)

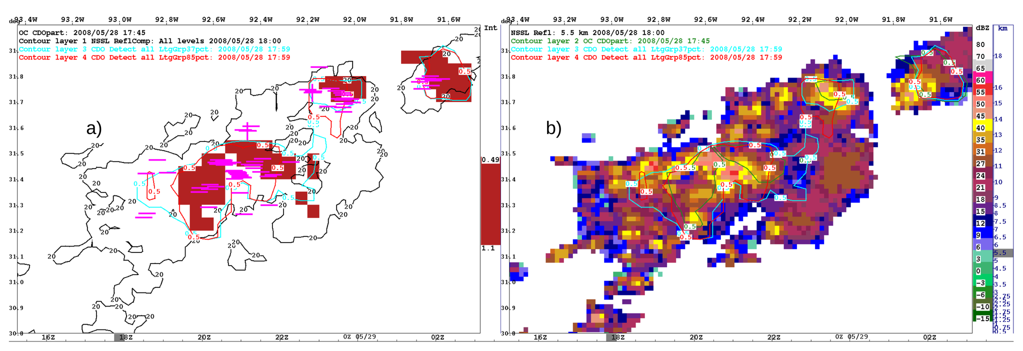

Figure 7. The three CDO configurations from Fig. 6 are shown with a) the 20 dBZ composite reflectivity contour plus NLDN flashes and b) reflectivity at 5.5 km MSL. The CDO (Fig. 6a) is shown by red shapes in a) and green contours in b), while the CDO from Fig. 6b is contoured with cyan lines and the CDO from Fig. 6c is contoured with red lines.

Possible Relationships between Storm Reflectivity, Cloud-to-Ground Lightning and Turbulence

Turbulence is an aviation hazard that, each year, causes injuries to flight crews and passengers as well as damage to the aircraft, resulting in millions of dollars of losses to the aviation industry. Avoiding regions of convectively-induced turbulence (CIT; i.e., turbulence within and near convective storms) requires that pilots receive timely and accurate warnings of imminent turbulence occurrence. The NEXRAD Turbulence Detection Algorithm (NTDA; Williams et al., 2004) has been developed by the Federal Aviation Administration (FAA) Aviation Weather Research Program (AWRP) as a means to provide timely and accurate CIT warnings to pilots.

Briefly, the NTDA uses the Doppler spectrum width to estimate regions of in-cloud turbulence. For the 28 May 2008 case study, the NTDA results are shown at three times (Fig. 8). Note the frequent co-location of turbulence and NLDN lightning flashes within the storm. The time series analysis (Fig. 9 also incorporates Fig. 3) shows that the volume of turbulence that is light or greater increases as the storm reflectivity and number of CG flashes are also increasing (between ~1600-1800 UTC). The first CG lightning flash slightly precedes light turbulence occurrence at 10.0 km, suggesting its possible use as a precursor signature. During this storm growth period, the maximum $\varepsilon^{1/3}$ values increase to moderate (Fig. 9d) and remain near that level for the rest of the period. After 1800, the volume of $\varepsilon^{1/3}$ at values $\geq$0.15 m$^{2/3}$ s^{-1} follows the reduction in storm reflectivity volume. These preliminary results are encouraging for improving our understanding of turbulence production within convective storms, but more study is required.

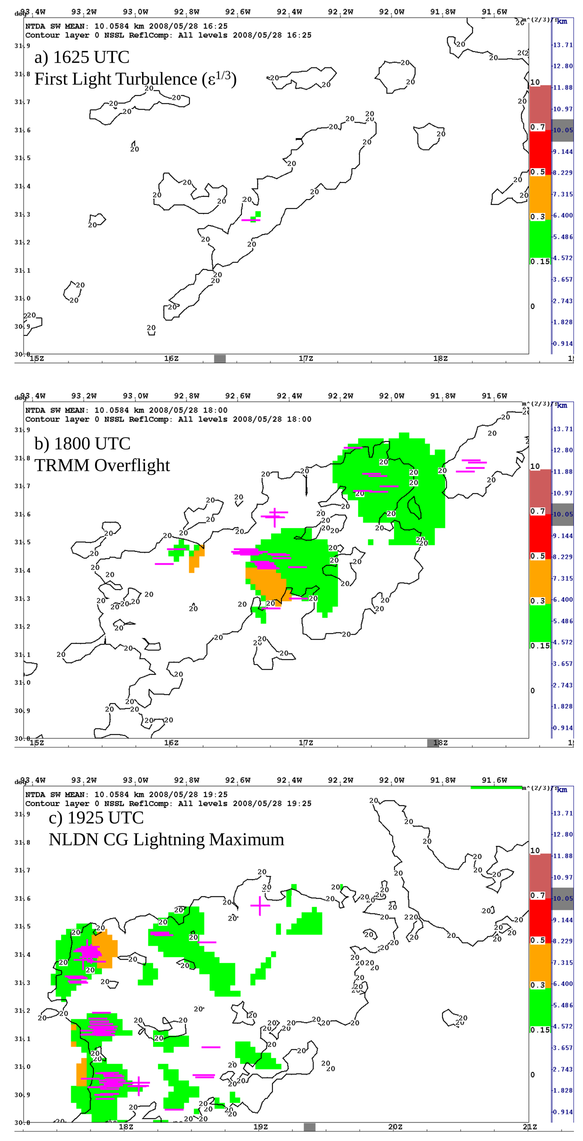

Figure 8. The eddy dissipation rate$^{1/3}$ ($\varepsilon^{1/3}$; m$^{2/3}$ s^{-1}) values are shown at the 10.05 km level from the NTDA along with the 20 dBZ contour from NSSL composite reflectivity (dBZ) and with the location of NLDN cloud-to-ground flashes at three times: a) 1625, b) 1800 and c) 1925 UTC on 28 May 2008. In a), light turbulence appears at the 10.05 km level 5 minutes after the first cloud-to-ground lightning flash (Fig. 3b). The $\varepsilon^{1/3}$ values are shaded such that green indicates light turbulence, orange indicates moderate, red is severe and maroon is extreme. The domain is shown in Fig. 1.

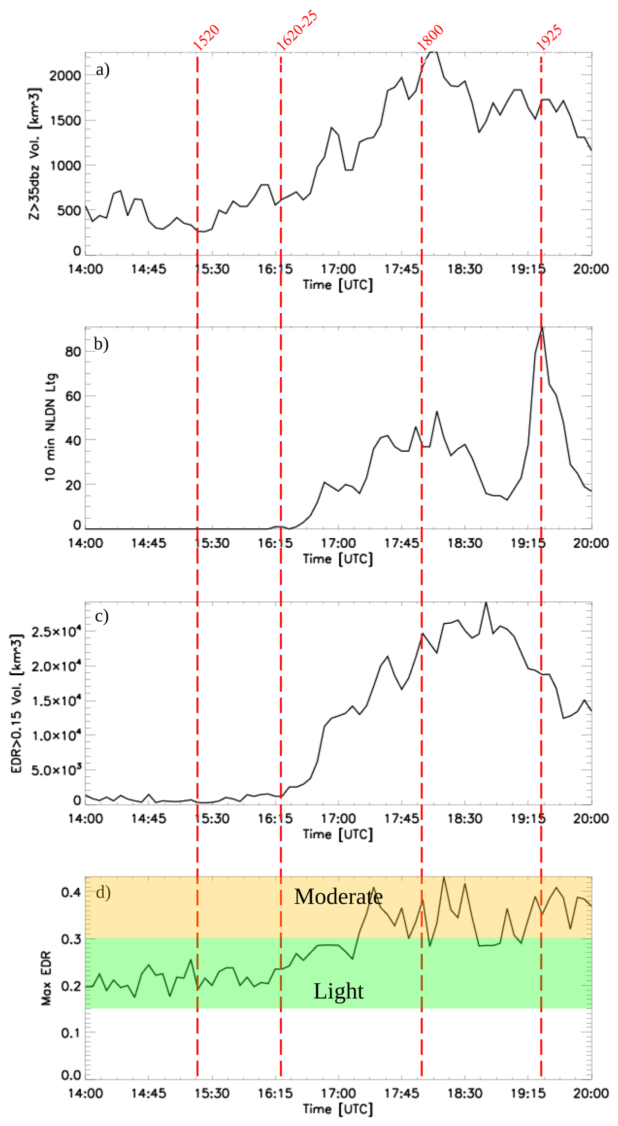

Figure 9. Similar to Fig. 3, time series plots from 1400 to 2000 UTC are shown. Fields plotted include a) the volume (km^3) of reflectivity $\geq$35 dBZ at and above the -10^{o}C level, b) the number of cloud-to-ground lightning flashes measured by the NLDN, c) the volume (km^3) of NTDA $\varepsilon^{1/3}$ values $\geq$0.15 m$^{2/3}$s^{-1} (light and greater turbulence) computed as a composite at and above the -10^{o}C level and d) the maximum $\varepsilon^{1/3}$ value at and above the -10^{o}C level within the domain. The times corresponding to Figs. 2 and 8 are shown by the vertical, red dashed lines.

Summary and Future Work

A case study has illustrated the use of advanced satellite and lightning products to better understand and detect hazardous convection. If a relationship between lightning and turbulence production is found and is found to be generally applicable, the launch of the Global Lightning Mapper (GLM) on GOES-R could provide an important diagnostic tool for locating regions of convectively-induced turbulence over the hemisphere and could vastly improve pilot awareness and avoidance of hazards. Use of GLM total lightning will be examined in the future with proxy data sets.

These preliminary results are promising but additional cases must and will be examined to ascertain the applicability of the results. Both oceanic and continental storms will be examined, although the NTDA mosaics are currently limited to the contiguous United States. Further, construction of a "hazard map" will be undertaken such that aviation hazards associated with convection can be summarized on one chart.

References

Blyth, A. M., H. J. Christian, K. Driscoll, A. Gadian, and J. Latham (2001), Determination of ice precipitation rates and thunderstorm anvil ice contents from satellite observations of lightning, Atmos. Res., 59– 60, 217–229.

Cecil, D.J., E.J. Zipser and S.W. Nesbitt, 2002: Reflectivity, ice scattering, and lightning characteristics of hurricane eyewalls and rainbands. Part I: Quantitative description. Mon. Wea. Rev., **130**, 769-784.

Kessinger, C., H. Cai, N. Rehak, D. Megenhardt, M. Steiner, R. Bankert, J. Hawkins, M. Donovan and E.R. Williams, 2010: A decision support system for diagnosing and nowcasting oceanic convection for oceanic aviation use. 17th Conf. Satellite Meteorology and Oceanography, paper 9.6.

Petersen, W.A., H.J. Christian and S.A. Rutledge, 2005: TRMM observations of the global relationship between ice water content and lightning. G. Res. Letters, **32**, L14819, doi: 10.1029/2005GL023236, 4 pages.

Spencer, R.W., H.M. Goodman, and R.E. Hood, 1989: Precipitation retrieval over land and ocean with the SSM/I: Identification and characteristics of the scattering signal. J. Atmos. Oceanic Technol., **6**, 254-273.

Williams, J.K., L. Cornman, D. Gilbert, S.G. Carson and J. Yee, 2004: Remote detection of turbulence using ground-based Doppler radars. 11th Conf. Aviation, Range and Aerospace, Amer. Meteor. Soc., 4-7 October 2004.

Acknowledgements

This research is supported by the National Aeronautics and Space Administration (NASA), primarily under Grants No. NNX09AM77G, NNA07CN14A and NNX08AL89G. Any opinions, findings, and conclusions or recommendations expressed in this material are those of the authors and do not necessarily reflect the views of NASA. The FAA AWRP is thanked for providing the NSSL radar mosaic and the NTDA data. The National Center for Atmospheric Research is sponsored by the National Science Foundation.